Phys. Med. Biol. 42 (1997) 2193–2213. Printed in the UK PII: S0031-9155(97)81387-5

An investigation into the effect of input function shape and image acquisition interval on estimates of washin for dynamic cardiac SPECT

Steven G Ross§, Andy Welch†‡, Grant T Gullberg‖ and Ronald H Huesman¶

§ University of Utah, Salt Lake City, UT, USA
¶ Lawrence Berkeley National Laboratory, University of California, Berkeley, CA, USA

Received 27 January 1997, in final form 20 May 1997

Abstract. Dynamic cardiac SPECT and PET can be used to measure myocardial perfusion by estimating the kinetic rate constant describing the washin of radioactive-labelled tracers from the blood to the extravascular myocardial tissue. Because of differences in photon statistics and data acquisition techniques, protocols which produce optimal estimates of the washin for dynamic cardiac PET may give suboptimal estimates if applied in dynamic cardiac SPECT. Two important factors in the estimation of washin are the shape of the tracer input function and the image acquisition interval. This study uses computer simulations to investigate the effect of varying the tracer infusion length and image acquisition interval on the bias and variance of estimates of washin obtained with dynamic cardiac SPECT and ^{99m}Tc-labelled teboroxime. Bias in parameter estimates can be introduced by aliasing, integration of the time-varying radioactivity by the detector, and detector motion. This bias can be reduced by decreasing the acquisition interval and using a longer-duration input function. However, this results in poor photon statistics, which generate large variance, and can also introduce bias in the estimates of the washin. Our studies indicate that better estimates of the washin are obtained by using an acquisition interval that is of sufficient duration to obtain adequate photon statistics even if this is at the expense of temporal resolution. The increase in bias caused by using a 10 or 20 s acquisition interval instead of a 5 s acquisition interval is minimal when compared with the reduction in variance. Variance in estimates is also reduced by using a sharp input function, resulting in higher peak counts during washin. It is also shown that the variance of estimates of the washin increases generally when faster kinetics are observed. This variance can, however, be reduced by using longer acquisition intervals.

1. Introduction

Single-photon emission computed tomography (SPECT) is used to infer variation in cardiac perfusion through visual interpretation of static images. It is possible, however, to obtain measurements of myocardial perfusion by tracking the kinetics of the radioactive-labelled tracer as it passes through the heart. Measures of myocardial perfusion are obtained by using dynamic imaging to estimate the kinetic parameters describing the exchange of radioactive-labelled kinetic tracers between the blood and the myocardial tissue. Estimates of these kinetic parameters are correlated to perfusion and may give more sensitive measurements

‡ Andy Welch is presently at the University of Aberdeen, Scotland.
‖ Please send correspondence to Grant T Gullberg, PhD, Department of Radiology, Medical Imaging Research Laboratory, AC-213 Medical Center, University of Utah, Salt Lake City, UT 84132, USA.

0031-9155/97/112193+21$19.50

of ischaemia than visual interpretation of static images. Dynamic positron emission tomography (PET) has been shown to be effective for estimating kinetic rate constants (Muzik et al 1993, Herrero et al 1992, Bergmann et al 1989, Mullani et al 1983), while dynamic SPECT also can be used to estimate kinetic parameters (Smith and Gullberg 1994, Smith et al 1994, 1996). Dynamic SPECT does, however, suffer from certain disadvantages when compared to dynamic PET. These include poor resolution (Welch et al 1995), large effects from photon attenuation (Gullberg et al 1985, Smith and Gullberg 1994), and increased blurring from geometric point response (Zeng et al 1991, Zeng and Gullberg 1992). All of the aforementioned effects can introduce bias into estimates of myocardial perfusion.

Another major drawback to dynamic cardiac SPECT is poor photon statistics which introduce large variances into the estimates. SPECT has poorer photon statistics than PET in large part because of the need for detector collimation, which severely decreases the number of detected photons. Photon statistics are further degraded in dynamic SPECT because of the need to acquire sufficient temporal information to adequately track the time-varying dynamics of the radioactive labelled tracer. In a typical static SPECT scan, projection data are obtained over 360° in approximately 20–30 min. In order to track the time-varying tracer, dynamic SPECT usually requires acquisition of 360° projection data in approximately 5–40 s, over a total duration of 10–15 min. This results in much poorer photon statistics in each dynamic projection set.

The poor photon statistics associated with these short acquisition intervals are evident from ongoing canine studies being carried out by this research group. In these studies, a three-detector SPECT system is used to track these dynamic changes. To do this, the camera gantry is rotated at high rates with the maximum rotation rate giving 360° coverage in 5 s. Five second acquisitions are then acquired for a duration of 15 min after the injection of teboroxime. In a dog weighing approximately 35 kg, a bolus injection of 15 mCi ^{99m}Tc-labelled teboroxime yields approximately 320 000 counts in the maximum 5 s projection set (64 × 64 × 60 angles). Welch et al (1995) demonstrated that kinetic parameter estimates are severely degraded when count levels approach these low ranges. It was shown, however, that slight improvements in count levels, e.g., from 320 000 counts in the maximum projection set (5 s acquisition intervals) to 640 000 counts, result in significant reduction in the variance of the kinetic parameter estimates.

Photon statistics can be improved by increasing the dose of ^{99m}Tc-labelled teboroxime. However, there are limits on photon counts set by injection levels of the radioactive-labelled tracer, the counting rates of the camera, and other count-limiting factors such as body attenuation. Once count rates have been maximized within these limits, count rates can be further improved by increasing the image acquisition interval (slowing the detector gantry). Another and perhaps more optimal approach would be to increase count rates by summing projection data from several acquisitions.

Increasing the acquisition interval by slowing the detector gantry adversely affects temporal resolution by not adequately sampling the time-varying dynamics of the tracer. Aliasing arises from insufficient sampling of the time-varying tracer. To reduce aliasing the acquisition interval can be decreased, resulting in better sampling, or the infusion can be dispersed over time, resulting in a smoother time-varying activity with less high-frequency content. The disadvantage of both of these techniques is that they result in fewer peak counts in the dynamic projection sets, which in turn results in less accurate kinetic parameter estimates.

Another effect which introduces bias into kinetic parameter estimates is the relative starting point of the time–activity curves with respect to the acquisition interval of the

photon detector over each dynamic sampling period. The counts in each projection bin are not an instantaneous sample of the tracer, but rather are the result of photons detected over a nite time interval. Thus, the sampled points are actually the result of integration of the tracer and each acquired sample in the detector is the integral of all counts in the acquisition period. This causes the kinetic parameter estimates to be sensitive to the time at which the tracer is injected with respect to the time at which the detector begins acquiring data.

The rotation of the gantry also affects the kinetic parameter estimates. Data inconsistencies arise because the tracer activity and the projection angle are changing as data are being acquired. Detector motion is speci c to the rotating gantry systems and can be avoided by using a static ring system. Static ring detector systems are commonly utilized in dynamic PET and have been introduced in dynamic SPECT (Stewart *et al* 1990); however, their use in SPECT is not widespread due to the cost and their limited number of applications.

This paper describes a study which investigates the effect of input function infusion length and image acquisition interval on the bias and variance of estimates of the washin of ^{99m}Tc-labelled teboroxime from the blood to the myocardial tissue obtained with dynamic cardiac SPECT. There have been research efforts investigating the effect of input function shape and acquisition interval on kinetic parameter estimation in dynamic PET (Mazoyer et al 1986, Cunningham and Jones 1993, Herrero *et al* 1989). However, dynamic cardiac SPECT suffers from much poorer photon statistics than those observed in dynamic cardiac PET. Because of this, protocols which produce optimal estimates of washin for dynamic PET may give suboptimal estimates if applied in dynamic cardiac SPECT. Also, detector motion can introduce bias which would not be present in dynamic PET studies. Computer simulations are carried out to study the effects of input function shape and image acquisition interval on aliasing, integration, detector motion, and photon statistics.

2. Background

To track the time-varying activity of the radioactive-labelled tracer injected into the body, dynamic projection sets are acquired over a nite period of time which is suf cient to view the temporal changes of the tracer. In experiments in our laboratory, the projections are acquired from a triple-detector SPECT system in which the detector gantry can be rotated through 120 in as little as 5 s to provide 360 angular coverage. Generally, 5 or 10 s rotation rates have been employed in our investigations. Projection sets are acquired over 15 min, resulting in 90{180 dynamic projection sets, depending on the gantry rotation rate. Dynamic images are then reconstructed from these projection sets using the expectation-maximization{maximum-likelihood (EM{ML) algorithm (Shepp and Vardi 1982, Lange and Carson 1984).

Of interest is the time-varying activity in the ventricular blood pool and localized regions of the myocardial tissue. The activity in these locations is determined by drawing regions of interest (ROIs) on the reconstructed images and sampling the tracer activity in these ROIs for each dynamic image. A one-compartment model is used to relate the time{activity curves in the blood and myocardium ROIs to the exchange of tracer between the blood and myocardial tissue. This exchange between the blood concentration $B(t)$ and the tissue concentration $C(t)$ is modelled with the kinetic parameters k_{21} (washin) and k_{12} (washout) with units of millilitres per minute per millilitre of extravascular space using the following differential equation:

$$\frac{d}{dt}C(t) = k_{21}B(t) - k_{12}C(t) \qquad (1)$$

with solution

$$C(t) = k_{21} \int_0^t e^{-k_{12}} B(t - \tau)\, d\tau. \quad (2)$$

Equation (2) states that the tissue concentration is a convolution of the blood activity and an exponential kernel which is a function of the rate constants. The tracer activity in the myocardium region of interest depends not only on the tissue activity, but also on the fraction of blood f_v that is present in the tissue, e.g., in the capillaries. Also, the activity cannot be sampled instantaneously, but rather is sampled over integrated time periods which are equal to the image acquisition interval (the rate of rotation of the SPECT system). Taking these factors into account, the total activity $A(t)$ in the tissue ROI is written as

$$A(t) = (1/\Delta t) \int_{t-\Delta t}^{t} \left[f_v + k_{21} \int_0^{t} e^{-k_{12}} B(t - \tau)\, d\tau \right] dt. \quad (3)$$

Given blood and tissue time–activity curves $B(t)$ and $A(t)$, as well as the acquisition interval Δt, the kinetic parameters k_{21}, k_{12}, and the blood fraction f_v are estimated with RFIT (Coxson *et al* 1992, Huesman and Mazoyer 1987, Huesman *et al* 1995). RFIT uses weighted least squares to estimate kinetic parameters from computational models with the form of equation (3) and, if necessary, for a noisy input function.

RFIT requires for input the curves $B(t)$ and $A(t)$ and the variance of $B(t)$ and $A(t)$, as well as the covariance between $B(t)$ and $A(t)$. In this paper the estimated blood and tissue variances are approximated to be equal to the ROI counts. This estimate is expected to be proportional to the error on the reconstructed count density using the EM–ML algorithm, although it does not represent the true errors in the ROI (Wilson and Tsui 1993, Barrett *et al* 1994, Wilson *et al* 1994). The tissue–blood covariances are estimated to be zero in this analysis. An incorrect estimate of the ROI variance and blood–tissue ROI covariance generally gives rise to an increase in the bias and variance associated with the kinetic parameter estimates (Gullberg *et al* 1997, Huesman and Mazoyer 1987).

Once estimates of the kinetic parameters are obtained, they can be used to obtain an estimate of flow multiplied by extraction in the myocaridal tissue. This measure can then be correlated to flow. Washin k_{21}, has been shown to be correlated to myocardial perfusion in dynamic cardiac SPECT (Smith and Gullberg 1994, Smith *et al* 1994, 1996). The parameter k_{12} is also correlated to flow; however, this correlation is not as strong as that seen in k_{21}. Because of this, the results presented in this paper will focus only on the parameter k_{21}.

3. Methods

The clinical dynamic SPECT system to be modelled consists of three detectors which are each rotated through 120° (360° coverage) to acquire each dynamic projection set. The detector can be rotated at different speeds; consequently the acquisition interval can be varied, with a minimum 120° rotation time of 5 s. Four different acquisition intervals are studied: 5, 10, 20, and 40 s. Four tracer infusion lengths are also studied: a bolus and 30, 60, and 90 s infusions. Sections 3.1 and 3.2 analyse ideal input functions which are not obtained from tomography, while sections 3.3 and 3.4 analyse input functions obtained from reconstructed tomographic images.

3.1. Aliasing

Effects due to undersampling of the blood and tissue time–activity curves are addressed first. The time–activity curves are based on canine studies by Smith *et al* (1994) with the

tracer time{activity in the blood pool for a bolus infusion modelled as

$$B(t) = \begin{cases} 450\,t/20 & t \leqslant 20 \\ 400\,e^{-0.1(t-20)} + 50\,e^{-0.001(t-20)} & t > 20. \end{cases} \quad (4)$$

Blood time{activity curves for 30, 60, and 90 s infusions are simulated by convolving equation (4) with 30, 60, and 90 s step functions, respectively. The myocardial tissue activity is simulated with kinetic values typical of those observed in a resting dog with $f_v = 0.15$, $k_{21} = 0.8\ \text{min}^{-1}$, and $k_{12} = 0.4\ \text{min}^{-1}$. Kinetic rate constants typical of those observed in a dog vasodilated with adenosine were also used with $k_{21} = 4.0\ \text{min}^{-1}$, $k_{12} = 2.0\ \text{min}^{-1}$, and $f_v = 0.15$. The frequency spectra of the time{activity curves are determined with an analytic Fourier transform of the time{activity curves. The spectra are used to demonstrate the aliasing associated with the time{activity curves. To simulate the nite acquisition period of the photon detector, the time{activity curves are sampled every 0.031 25 ($\frac{1}{32}$) s and these values are integrated over nite intervals which correspond to the acquisition interval of the detector (5, 10, 20, and 40 s). The integrated data are used in RFIT to estimate the kinetic parameters k_{21}, k_{12}, and f_v.

3.2. Photon integration

Each data point that is used in the estimation of the kinetic parameters is the integral of the continuously varying time{activity curve. This integration can potentially result in a misrepresentation of the actual time{activity curve and subsequently introduce bias into kinetic parameter estimates. The misrepresentation of the signal is most severe when the integration period of the detector ends near the peak of the input function. This causes the peak of the input function to be represented by approximately equal points on either side of the peak. This misrepresentation of the signal can potentially introduce bias into kinetic parameter estimates. This causes the kinetic parameter estimates to be dependent on any time shift of the time-varying tracer with respect to the integration period of the detector, which could occur by not properly timing the injection and the starting point of the acquisition. A reduction in bias can be achieved by optimizing the starting time point of the tracer infusion with respect to the starting acquisition interval of the detector. This effect is investigated by shifting the starting point of the time{activity curves to optimize the parameter estimates. The input functions are shifted by quarter intervals of the acquisition interval to obtain optimum estimates of washin. Delay intervals of 0, 1.25, 2.5, and 3.75 s are used for 5 s acquisitions; delay intervals of 0, 2.5, 5.0, and 7.5 s are used for 10 s acquisitions; delay intervals of 0, 5, 10, and 15 s are used for 20 s acquisitions; and delay intervals of 0, 10, 20, and 30 s are used for 40 s acquisitions.

3.3. Detector motion

The next group of simulations addresses effects from tomography and detector motion. These simulations model a clinical three-detector SPECT system. The geometry is modelled with a modi ed version of the MCAT heart and torso phantom (Tsui *et al* 1994, Terry *et al* 1990). A single transaxial slice of the phantom is shown in gure 1. The phantom consists of three regions; myocardial tissue, blood pool, and a uniform background with 20% of the activity in the blood pool. Time-varying activity in the phantom is simulated with the time{activity curves corresponding to a bolus infusion and a 90 s infusion. The MCAT phantom is discretized into 128 128 pixels and 60 angular unattenuated fan beam projections are formed with a ray-driven, line-length weighting projector (Huesman *et al* 1977). The

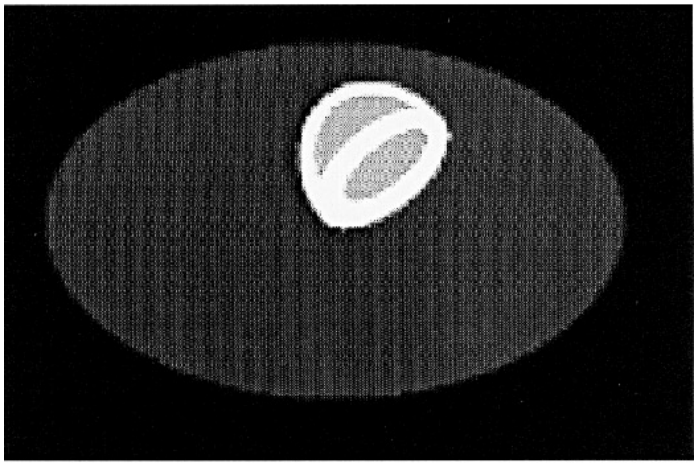

Figure 1. A transaxial slice of the MCAT phantom used in the simulations to generate the emission data.

projections are discretized into 128 2 bins which are subsequently binned to 64 1. The size of each pixel is 0.712 cm, the radius of rotation is 34 cm, and the centre of rotation is at the centre of the phantom. Because of the fan beam geometry, the projection data truncates 32% of the MCAT phantom.

Each of the 60 projections in a 360 tomographic set is the average of a certain number of subprojections (over six degrees). To simulate the varying image acquisition intervals (360 detector rotation time), each subprojection is obtained every 0.03125 s; however, the number of subprojections per 6 angular bin is varied. Thus a 5 s image acquisition interval used eight subprojections per 6 angular bin, a 10 s interval used 16 subprojections, a 20 s interval used 32 subprojections, and a 40 s interval used 64 subprojections. The 60 projections are then used to reconstruct a 64 64 transaxial image with the expectation-maximization{maximum-likelihood algorithm (EM{ML) (Shepp and Vardi 1982, Lange and Carson 1984). The bias in the parameter estimates is observed as a function of the number of iterations of the EM{ML algorithm. The projection data are also reconstructed using filtered backprojection with a ramp filter with cutoff frequency of 0.5 cycles/projection bin. Filtered backprojection is used for comparison purposes with the EM{ML algorithm; however, it is not used when photon noise is included in the simulations. A single transaxial slice is used to draw blood and tissue ROIs. The blood ROI is 7.2 cm^3 and the tissue ROI is 4.2 cm^3.

3.4. Photon statistics

Poisson noise is added to the projection sets to simulate the statistics observed in canine studies in our laboratory. In these studies, an injection of 15 mCi ^{99m}Tc-labelled teboroxime resulted in approximately 320 000 counts in the maximum 360 projection set over the 10 min dynamic acquisition, while injections of 30 mCi ^{99m}Tc-labelled teboroxime resulted in approximately double these counts.

Blood and tissue time{activity curves are obtained from dynamic images reconstructed with 25 iterations of EM{ML using the moving detector system and the MCAT phantom. The projection data are generated as described in section 3.3. Poisson noise is added to each projection set with a scaling factor set to ensure that the appropriate statistics were observed for all acquisition intervals and input functions. In all cases one hundred

realizations were performed with different seeds used for the random number generator. Estimates are obtained for each realization and the results show the population mean of these estimates along with the population standard deviation. In addition, the variance in the estimates is plotted against the absolute bias.

4. Results

The results of sections 4.1 and 4.2 were calculated with integration of the exact blood and tissue time{activity curves. The results of sections 4.3 and 4.4 were calculated using simulated projection data of the MCAT phantom. In sections 4.3 and 4.4, estimates are obtained using time{activity curves obtained from ROI analysis on reconstructed transaxial slices of the MCAT phantom.

4.1. Aliasing

The blood and tissue time{activity curves are shown in gure 2(a){(c). The Fourier transforms of these curves are shown in gure 3(a){(c) respectively. The vertical lines correspond to the frequency that could be recovered for a given acquisition interval (5, 10, 20, or 40 s) based on Nyquist's theorem. For example, an acquisition interval of 5 s can recover frequencies below $=.2$ 5 s). The frequency spectra of gure 3(a) show that the vast majority of the blood signal is recovered hw 5 s acquisition intervals. Higher frequencies of the bolus infusion are lost with 10 s acquisitions, and a signi cant amount of the spectrum is lost with 20 and 40 s acquisitions. As the infusion is lengthened, a much smaller portion of the frequency response is lost.

Figure 3(b) and (c) shows the frequency spectra for the tissue curves. The majority of the frequency components are recovered for 5 and 10 s acquisitions using resting parameters. There are substantial frequency components lost with 20 and 40 s acquisition intervals, particularly for the bolus and 30 s infusions. The frequency spectrum of the vasodilated tissue curve shows that a much greater portion of the signal is lost than in the resting case.

Figure 4 shows estimates of k_{21} for the resting kinetic parameters. The results are obtained by integrating the time{activity curves over the acquisition interval and using RFIT to obtain estimates of k_{21}. The plot shows that the most accurate estimates are obtained with 5 s acquisitions, with bias increasing as the acquisition interval is increased. In general, bias is maximum for a bolus infusion because the aliasing is greatest, while the least bias is seen with a 90 s infusion. There are apparent anomalous results for 20 and 40 s acquisition intervals. For instance, when a bolus infusion is simulated, the bias in washin of a 20 s acquisition is greater than that of a 40 s acquisition. Also, the bias for the 30 s infusion is disproportionately large with 40 s acquisition intervals for the resting parameters. These anomalies are due to integration effects which are related to the shape of the input fraction.

4.2. Photon integration

As mentioned in section 3.2, integration of the time{activity curve by the detector can introduce bias into the kinetic parameter estimates. The sampled version of the time{activity curve can vary depending on the duration of the acquisition interval and the time at which the acquisition interval begins relative to the starting point of the input function. This effect could be reduced by shifting the input function in time, in order to optimize the injection of tracer with respect to the detector acquisition interval.